HHS Public Access

Author manuscript

Synapse. Author manuscript; available in PMC 2020 October 30.

Published in final edited form as:

Synapse. 2018 September ; 72(9): e22042. doi:10.1002/syn.22042.

Kappa Opioid Receptor Binding in Major Depression: A Pilot Study

Jeffrey M. Miller, M.D.[1,2], **Francesca Zanderigo, Ph.D.**[1,2], **Priya D. Purushothaman, B.S.**[2], **Christine DeLorenzo, Ph.D.**[4], **Harry Rubin-Falcone, B.A.**[1,2], **R. Todd Ogden, Ph.D.**[1,3], **John Keilp, Ph.D.**[1,2], **Maria A. Oquendo, M.D., Ph.D.**[5], **Nabeel Nabulsi, Ph.D.**[6], **Yiyun H. Huang, Ph.D.**[6], **Ramin V. Parsey, M.D., Ph.D.**[4], **Richard E. Carson, Ph.D.**[6], **J. John Mann, M.D.**[1,2]

[1.]Division of Molecular Imaging and Neuropathology, New York State Psychiatric Institute, New York, NY

[2.]Department of Psychiatry, Columbia University, New York, NY

[3.]Department of Biostatistics, Mailman School of Public Health, Columbia University, New York, NY

[4.]Department of Psychiatry and Behavioral Science, Stony Brook University School of Medicine

[5.]Department of Psychiatry, Perelman School of Medicine, University of Pennsylvania

[6.]Department of Radiology and Biomedical Imaging, Yale University School of Medicine

Abstract

Endogenous kappa opioids mediate pathological responses to stress in animal models. However, the relationship of the kappa opioid receptor (KOR) to life stress and to psychopathology in humans is not well described. This pilot study sought, for the first time, to quantify KOR in major depressive disorder (MDD) *in vivo* in humans using PET imaging. KOR binding was quantified *in vivo* by PET imaging with the [^{11}C]GR103545 radiotracer in 13 healthy volunteers and 10 participants with current MDD. We examined the relationship between regional [^{11}C]GR103545 total volume of distribution (V_T) and diagnosis, childhood trauma, recent life stress, and, in a subsample, salivary cortisol levels during a modified Trier Social Stress Test (mTSST), amygdala, hippocampus, ventral striatum and raphe nuclei. Whole-brain voxel-wise analyses were also performed. [^{11}C]GR103545 V_T did not differ significantly between MDD participants and healthy volunteers in the 4 *a priori* ROIs (p=0.50). [^{11}C]GR103545 V_T was unrelated to reported childhood adversity (p=0.17) or recent life stress (p=0.56). A trend-level inverse correlation was observed between [^{11}C]GR103545 V_T and cortisol area-under-the curve with respect to ground during the mTSST (p=0.081). No whole-brain voxel-wise contrasts were significant. Regional [^{11}C]GR103545 V_T, a measure of *in vivo* KOR binding, does not differentiate MDD from healthy

Corresponding author: Jeffrey M. Miller, M.D., 1051 Riverside Drive #42, New York, NY 10032, jm2233@cumc.columbia.edu, fax: (888) 971-4305.

Conflicts of Interest/Financial Disclosures:

Drs. Miller, Purushothaman, Zanderigo, DeLorenzo, Nabulsi, Ogden, Keilp, Carson, Huang and Parsey, as well as Mr. Rubin-Falcone, report no conflicts of interest. Dr. Oquendo receives royalties for the commercial use of the C-SSRS. Her family owns stock in Bristol Myers Squibb. She received a stipends from the American Psychiatric Association for her roles as president elect and president. Dr. Mann receives royalties for commercial use of C-SSRS from Research Foundation for Mental Hygiene.

volunteers in this pilot sample. Future studies may examine KOR binding in subgroups of depressed individuals at increased risk for KOR abnormalities, including co-occurring mood and substance use disorders, as well as depression with psychotic features.

Keywords

kappa opioid receptor; dynorphin; stress; cortisol; PET imaging; mood disorders

Introduction

Depression is the leading cause of disability and a significant cause of mortality globally (WHO, 2017), yet current understanding of its pathophysiology remains incomplete. Many patients suffering from major depressive disorder (MDD) do not achieve complete remission after multiple trials of currently available antidepressant medications (McGrath and Miller, 2015). Identification of novel molecular targets in depression is essential to improve treatment success.

The kappa opioid system mediates maladaptive responses to stress in animal models. As life stress represents a significant risk factor for MDD (Nemeroff and Vale, 2005), the kappa opioid system may represent a possible molecular target for the treatment of mood disorders in humans, particularly for episodes that develop in the context of life stress. Endogenous kappa opioids, dynorphins, are released in response to laboratory stress (Land et al., 2008), an effect mediated by corticotropin releasing factor (CRF) (Bruchas et al., 2009), placing dynorphin release downstream of hypothalamic-pituitary-adrenal (HPA) axis activation. Dynorphins bind selectively to the kappa opioid receptor (KOR), leading to downstream effects on neurochemical systems implicated in MDD. Specifically, KOR stimulation lowers extracellular levels of dopamine in nucleus accumbens (NAc) (Carlezon et al., 2006); and these effects on reward circuitry could contribute to anhedonia. In addition, KOR stimulation inhibits norepinephrine release from locus ceruleus following sensory stimuli (Kreibich et al., 2008) and inhibits serotonin release in raphe nuclei, neocortex and nucleus accumbens (Berger et al., 2006; Tao and Auerbach, 2002).

Animal models of depression suggest that inhibition of KOR may have an antidepressant effect (Mague et al., 2003; McLaughlin et al., 2006; McLaughlin et al., 2003; Newton et al., 2002; Shirayama et al., 2004). Conversely, KOR agonists *increase* the depression-like phenotype in animal models (Carlezon et al., 2006; Mague et al., 2003). Genetic manipulation studies support these pharmacological studies (McLaughlin et al., 2006; McLaughlin et al., 2003), suggesting that dynoprhin release (and KOR stimulation) is required for expression of the depression-like phenotype in the setting of stress.

Despite compelling evidence linking KOR signaling to depression-like symptoms in animals, and clinical development of KOR antagonists (Ehrich et al., 2015), the kappa opioid system remains understudied in humans with mood disorders. One previous PET study used the KOR antagonist radiotracer [^{11}C]LY2795050 to quantify KOR total distribution volume (V_T) in 30 trauma-exposed individuals with a range of psychiatric diagnoses and 5 non-trauma-exposed healthy volunteers, and reported inverse correlations

between [^{11}C]LY2795050 V_T and a composite measure of depression and anxiety symptoms in amygdala, anterior cingulate, and ventral striatum. This effect was mediated by 24-hour urinary cortisol levels (Pietrzak et al., 2014). This is consistent with life stress elevating dynorphin, leading to compensatory KOR down-regulation, as has been observed *in vitro* (Chen et al., 2006; Jordan et al., 2000; Li et al., 2003) and *in vivo* (Wang et al., 2009), and with the stimulation of dynorphin release by HPA-axis activation (Bruchas et al., 2009). An alternative interpretation of low KOR binding in the setting of a high dynorphin state would be reduced radiotracer binding due to competition with endogenous dynorphin itself.

In this study, we used a KOR agonist radiotracer, [^{11}C]GR103545 (Naganawa et al., 2014; Talbot et al., 2005), to quantify KOR binding in individuals with current MDD and healthy volunteers. [^{11}C]GR103545 is highly specific for KOR (Schoultz et al., 2010) but suffers from slow kinetics (Tomasi et al., 2013), complicating quantification. [^{11}C]GR103545 has been used in PET studies in rats to quantify acute occupancy by the KOR agonist salvinorin, as well as persistent KOR agonist-mediated receptor downregulation (Placzek et al., 2015). Consistent with these findings, recent human data suggest that [^{11}C]GR103545 may be sensitive to endogenous dynorphin in cocaine-use disorder (Diana Martinez, personal communication). Test-retest studies of this radiotracer demonstrate moderate test-retest reliability of ~15%, and blocking studies demonstrate specific binding in all brain regions examined, preventing the use of reference-region-based approaches (Naganawa et al., 2014).

This pilot study of *in vivo* KOR binding using PET imaging and the agonist radiotracer [^{11}C]GR103545 enrolled individuals with current MDD and age- and sex-matched healthy volunteers. We examined the relationship of KOR binding to depression severity, reported childhood adversity, and recent life stress. We hypothesized that: 1) [^{11}C]GR103545 V_T would be lower in individuals with current MDD as compared to a healthy volunteer sample in four *a priori* regions of interest (ROIs) in which KOR activation occurs in animal studies in response to stress (Land et al., 2008): nucleus accumbens, amygdala, hippocampus, and raphe nuclei; and 2) both early and recent life stress would be inversely correlated with [^{11}C]GR103545 V_T in these same ROIs. Given that KOR activation occurs in response to HPA axis activation, an exploratory analysis examined the correlation between regional [^{11}C]GR103545 V_T and HPA axis activation in a subset of individuals, using a modified Trier Social Stress Test (mTSST). We hypothesized a negative relationship between [^{11}C]GR103545 V_T and HPA activation. Within the MDD group, we also explored the relationship between [^{11}C]GR103545 V_T and depression severity. Whole-brain voxel-wise analyses were conducted to explore regions outside of the *a priori* ROIs.

Materials and Methods

Participants

Study procedures were approved by the Institutional Review Boards of The New York State Psychiatric Institute and the Yale University School of Medicine. Participants were recruited through online advertisements and clinician referrals. Eligibility assessment included medical and psychiatric history, physical examination, routine blood tests, urinalysis, and urine toxicology. Psychiatric diagnoses were established using the Structured Clinical Interview for DSM-IV (First et al., 1995), conducted by doctoral- or masters'-level

psychologists and reviewed in a consensus conference of research psychologists and psychiatrists.

14 individuals with MDD and 14 healthy volunteers enrolled in this study and completed MRI scanning. Of these, three MDD participants and one healthy volunteer did not complete PET scanning due to inability to place radial artery catheter. One additional MDD participant did not complete PET scanning due to radiotracer synthesis failure. We report data on a final analyzed sample of 10 MDD participants and 13 healthy volunteers.

Eligibility Criteria

Inclusion criteria for MDD individuals included: 1) Age 18–55; 2) MDD in a current depressive episode (MDE); 3) 17-item Hamilton Depression Rating Scale (HDRS) score ≥16 at time of consent; 4) If on current antidepressant medications, lack of significant benefit after trial of adequate dose and duration, and able to tolerate medication washout (although no participant was taking an antidepressant medication at the time of enrollment). Exclusion criteria for MDD individuals included: 1) unstable medical conditions; 2) pregnancy; 3) neurological disease or head trauma with evidence of cognitive impairment; 4) lifetime history of alcohol or substance abuse or dependence (other than nicotine); 5) lifetime history of psychotic illness, or anorexia or bulimia in the past year; 6) current use of opioid medication. Healthy volunteers had an absence of current or past DSM-IV Axis I diagnosis (though specific phobia was permissible), and met inclusion criterion 1) as well as all exclusion criteria listed for the MDD group.

Clinical Assessments

Depression severity was quantified with the HDRS (Hamilton, 1960) and the Beck Depression Inventory (BDI) (Beck et al., 1961). Suicide attempt history was assessed with the Columbia Suicide History Form (Oquendo et al., 2003). Suicidal ideation was quantified using the Beck Scale for Suicide Ideation (SSI) (Beck et al., 1979). Recent life stress was quantified using the Interview for Recent Life Events (IRLE) (Paykel, 1997), in which an interviewer surveys the occurrence of life events across a range of social and occupational domains that have occurred within the past six months. For each event elicited, the interviewer evaluates the objective negative impact and the extent to which the event is independent of illness on a five-point scale. We examined the number of life events of at least moderate negative impact in the past six months as a measure of recent life stress. Childhood trauma was quantified using the childhood trauma questionnaire (CTQ) (Bernstein and Fink, 1998). We used the total score of the CTQ as a measure of childhood trauma.

Cortisol responses to stress were quantified using the mTSST in a subset of individuals (5 healthy volunteers and 4 MDD participants). During the TSST (Kirschbaum et al., 1993), participants perform a 5-minute personal introduction speech and then complete a speeded mental arithmetic task over 9 minutes, in the presence of an examiner and an observer (“confederate”), a staff person not known by the subject, who provides negative feedback to the subject. This modified form of the TSST did not use explicit negative feedback, due to its initial use in children and in populations at high risk for suicide. Examiner and

confederate maintained neutral affect throughout TSST procedures. TSST procedures were performed during the afternoon in all participants. Cortisol was quantified in five saliva samples per subject that were obtained longitudinally 10 minutes prior to the stress procedure and then 15, 20, 30, and 40 minutes from initiation of the stressors. We analyzed total cortisol output, calculated as area under the curve with respect to ground (AUCG), and cortisol reactivity, using AUC with respect to increase (AUCi) (Pruessner et al., 2003). AUCs were computed with the trapezoid method using raw values. Natural logarithmic (ln) transformation was applied to AUC data as they were not normally distributed.

PET Acquisition

PET images were acquired at the Yale University PET Center on a Siemens HRRT PET camera. Head motion was recorded during the scan using a commercial optical tracking system, the Polaris Vicra system (Northern Digital Inc., Waterloo, ON, Canada). Images were reconstructed and corrected for attenuation, scatter, and motion using the MOLAR algorithm (Jin et al., 2013). Following acquisition of a transmission scan, [^{11}C]GR103545, a KOR-specific agonist radiotracer, was synthesized as previously described (Nabulsi et al., 2011), then injected intravenously as a single bolus (Table 1). [^{11}C]GR103545 was administered at tracer doses, with a stringent mass limit of ≤0.02 micrograms per kilogram of the subject's body weight (Tomasi et al., 2013). No physiological or psychological adverse effects of radiotracer injection were observed among participants in this study. Dynamic PET images were acquired in 3D mode over a period of 150 minutes using 36 frames of increasing duration. The scanning period of 150 minutes was chosen based on previous human studies (Naganawa et al., 2014); the high sensitivity of the HRRT PET camera permitted useable data to be acquired for this duration, despite the short half-life of ^{11}C. A metabolite-corrected arterial input function was quantified based on samples obtained during each scan as follows: before each PET scan, catheters were inserted in a forearm vein and a radial artery for radioisotope injection and arterial blood sampling respectively, as described in (DeLorenzo et al., 2015). Total radioactivity in the arterial blood samples was analyzed as described elsewhere (Ametamey et al., 2006). After correction for dispersion and delay, concentration values obtained in plasma samples and collected both automatically and manually were combined. The resulting data points were convolved with a Gaussian function (full-width half-maximum=24 s) to smooth the first 6 minutes of the combined curve. A high-performance liquid chromatography (HPLC) assay of 7 of the collected arterial blood samples provided levels of unmetabolized parent compound. These levels were fit with a Hill function (Wu et al., 2007). The metabolite-corrected arterial input function was obtained by multiplying the fitted parent fraction curve and the merged plasma counts, and fitting the resulting data points with a combination of a straight line (before the peak) and the sum of three decreasing exponentials (after the peak).

Magnetic Resonance Imaging (MRI) Acquisition

T1-weighted structural images were acquired on a Phillips 3T Achieva scanner acquiring 1 mm^3 isotropic voxel dimension with a TE of 2.98, TR of 6.59, flip angle of 8.0, and acquisition matrix of 256 × 256.

Image Processing

Raw MRI images were cropped utilizing Atropos to remove non-brain material (Avants et al., 2011a), and then segmented into gray, white, and CSF using SPM 5 (Ashburner and Friston, 2005). ROIs in this study were identified using an automated algorithm (Milak et al., 2010) that uses nonlinear registration techniques to warp 18 manually labeled MRI images to the target image as previously described (Milak et al., 2010). Four *a priori* ROIs were examined: amygdala, ventral striatum, hippocampus, and raphe nuclei (RN) (Land et al., 2008). Because the RN ROI cannot be reliably identified on MRI images, this region was labeled using a mask of the average location of the RN in 52 healthy subjects derived from PET data, using [^{11}C]WAY-100635 (specific for the serotonin 1A receptor) voxel binding maps warped into standard space, as described previously (Delorenzo et al., 2013).

The FMRIB linear image registration tool (FLIRT), version 5.0 (FMRIB Image Analysis Group, Oxford, UK) was used to correct for residual subject motion. PET-to-MRI transformations were computed using FLIRT as previously described (DeLorenzo et al., 2009). Time activity curves were generated by averaging measured activity in all voxels within a ROI over the time course of PET acquisition.

PET Outcome Measure Estimation

Graphical approaches such as multilinear analysis-1 (MA1) are recommended for optimal quantification of [^{11}C]GR103545 binding (Naganawa et al., 2014). Quantification of [^{11}C]GR103545 V_T was therefore performed at the ROI level using likelihood estimation in graphical approach (LEGA) (Ogden, 2003), a method with similar characteristics to MA1, and setting the t* (i.e., first time point of the linear phase) equal to 40 minutes after tracer injection, as previously described (Naganawa et al., 2014).

At the voxel-level, the radiotracer V_T was estimated using empirical Bayesian estimation in graphical analysis (EBEGA) (Zanderigo et al., 2010), a fully automatic approach that incorporates LEGA (Ogden, 2003) estimation of V_T in a Bayesian framework. EBEGA produces meaningful and useful voxel images by reducing the variability of the estimators, which are shrunk towards reasonable prior means. EBEGA determines its prior distributions in a fully automated way by using a two-step k-means clustering of grey matter voxel raw time activity curves to eliminate reliance of the estimators on subjectively chosen prior distributions. Once the prior distributions have been determined, a maximum a posteriori estimation is performed using for each voxel the prior of the cluster to which it belongs. Example unmodeled (standardized uptake value, SUV) and modeled (EBEGA) voxel images for a single participant whose mean V_T was at the median of the entire sample are demonstrated in Figure 1.

Statistical Analysis

To properly account for the covariance structure of the data, linear mixed-effects models were fit to the ROI-level V_T estimates with region and diagnostic group as fixed effects and subject as the random effect. Data were log-transformed to stabilize the variance, and because our principal hypothesis of a difference between groups specifies differences in each ROI that are proportional to each ROI's binding level. Log transformation has been used in

multiple PET studies by our group and others to address these issues. As the natural log is a monotone transformation, demonstrating a difference in log V_T is equivalent to demonstrating a difference (in the same direction) in V_T. Estimated binding values were weighted in the model according to estimated measurement error. Weights were determined based on standard errors computed using a bootstrap algorithm that takes into account errors in the PET time activity curve data (Ogden and Tarpey, 2006). Linear mixed effects models of binding, i.e., log V_T, (with region and diagnostic group as fixed effects and subject as the random effect) were fit using R 3.1.2 (http://cran.r-project.org). The relationships of other variables to KOR binding (CTQ, IRLE, TSST) were similarly examined using linear mixed effects modeling, as were the effects of possible covariates. Sex was included as a covariate in all analyses given a recent report of sex effects on kappa binding assessed by PET (Vijay et al., 2016); other covariates were also considered, including age, but not included in the final models. T-tests were performed in SPSS Statistics 18 (http://www.spss.com/software/statistics/).

Voxel-level Analysis

EBEGA PET images were warped into native MRI space using transforms generated during ROI analysis, then warped into standard space using Advanced Normalization Tools (Avants et al., 2011b). Images were smoothed with an 8 mm kernel and grey matter masked with a standard-space FSL-Toolbox template.

Voxel-level statistical analyses were performed in SPM8 (Institute of Neurology, University College of London, London, England) implemented in Matlab2012b (The Mathworks Inc, Natick, Mass). A two-sample t-test comparing V_T between MDD participants and healthy volunteers was performed. In MDD participants, correlations of V_T with BDI, 17-item HDRS, and IRLE were performed. Correlations of V_T with CTQ, AUCg and AUCi were performed considering MDD and healthy volunteers together with diagnosis as a covariate. For all analyses, an *a priori* cluster threshold was set to $p<0.01$ with an extent threshold of $p < 0.05$ after correction for multiple comparisons.

Results

Effect of Diagnosis

No difference was observed in [^{11}C]GR103545 V_T between MDD and healthy volunteer groups in the 4 *a priori* ROIs (Figure 2; F=0.48, DF=1,20, p=0.50). We also did not observe a region-by-diagnosis interaction (F=0.41, DF=3,63, p=0.75), indicating no regionally-specific difference in binding between MDD and healthy volunteer groups across the four ROIs.

Relationship to Depression Severity

We did not observe a relationship between KOR V_T and depression severity measured using the BDI (F=1.49, DF=1,7, p=0.26) or the 17-item HDRS (F=0.02, DF=1,7, p=0.89).

Effect of Life Stress:

We did not observe a relationship between reported childhood trauma quantified by the CTQ and [^{11}C]GR103545 V_T in the entire sample including diagnosis and sex as covariates (F=2.05, DF=1,16, p=0.17). Because only one healthy volunteer reported a life event of moderately negative impact during the six-month period prior to scanning, we examined recent life stress relationships to KOR binding within the MDD group only. We did not observe a relationship between [^{11}C]GR103545 V_T and the number of negative life events in the prior six months (F=0.37, DF=1,7, p=0.56).

Relationship to Cortisol Responses during TSST

We examined the effect of cortisol responses in the subset who completed the TSST, accounting for the effect of diagnosis and sex in the model. We observed a trend-level inverse relationship between *total* cortisol output during the TSST (AUC_G) and [^{11}C]GR103545 V_T (Figure 3; F=4.77, DF=1,5, p=0.081). No relationship was observed between cortisol *reactivity* (AUC_I) and [^{11}C]GR103545 V_T (F=0.86, DF=1,5, p=0.40).

Possible covariates:

We observed no relationship between [^{11}C]GR103545 V_T and potential covariates, including sex (F=0.57, DF=1,19, p=0.46) and age (F=0.00, DF=1,19, p=0.997).

Whole-Brain Voxel-wise Analyses

Whole-brain voxel-wise analyses with an *a priori* cluster threshold of $p<0.01$ and an extent threshold of $p < 0.05$ after correction for multiple comparisons yielded no effects of diagnosis, depression severity, early or recent life stress, or TSST cortisol AUC_G or AUC_I that survived these statistical thresholds.

Discussion

In this first pilot study quantifying KOR binding *in vivo* in MDD participants using PET with the KOR agonist radiotracer [^{11}C]GR103545, we did not observe a difference in [^{11}C]GR103545 V_T between MDD and healthy volunteer groups, nor did we observe relationships between [^{11}C]GR103545 V_T and measures of life stress or depression severity. However, consistent with our hypotheses, we did observe an inverse relationship between [^{11}C]GR103545 V_T and cortisol output during the TSST at a statistical trend level.

Diagnosis contrasts

Quantification of KOR in MDD was motivated by extensive animal literature identifying pro-depressant effects of KOR agonists and antidepressant effects of KOR antagonists (Carlezon et al., 2006; Mague et al., 2003; McLaughlin et al., 2006; McLaughlin et al., 2003; Newton et al., 2002; Shirayama et al., 2004), as well as by dysphoria-inducing effects of KOR agonists in humans (Pfeiffer et al., 1986). Moreover, another PET imaging study using the KOR antagonist radiotracer [^{11}C]LY2795050 observed an inverse correlation between [^{11}C]LY2795050 binding and a cluster of depressive and anxious symptoms in amygdala, anterior cingulate, and ventral striatum in a diagnostically heterogeneous group

(Pietrzak et al., 2014). Several possible explanations exist for the lack of an observed effect of MDD diagnosis on [^{11}C]GR103545 V_T in our current investigation. This pilot study was powered to detect only large effects. Moreover, KOR alterations may be confined to a stress-sensitive subsample of MDD, or more pronounced in MDD with psychotic features or psychomotor agitation, as these psychopathologies are associated with greater HPA axis activation (Keller et al., 2006; Schatzberg, 2015), which acts upstream from kappa opioid activation (Bruchas et al., 2009). Additionally, KOR agonists induce not just dysphoria but also psychosis in humans (Pfeiffer et al., 1986). There is also an extensive literature regarding kappa opioid abnormalities that contribute to stress-induced relapse to substance use disorders (Chavkin and Koob, 2016). Individuals with depressive symptoms during early abstinence from alcohol or recreational drugs are another subpopulation of depressed individuals likely to show KOR abnormalities.Neither of these groups was included in the current MDD sample, as we sought initially to examine the KOR system in relationship to depression alone. Our findings, if confirmed in large samples, would be relevant to clinical investigations of KOR antagonists or functional antagonists in depression (Ehrich et al., 2015), as it would suggest the importance of identifying subpopulations of depressed patients at greater risk for KOR abnormalities.

Relationship to cortisol measures from the TSST

Exploratory analysis in a subset of participants revealed a statistical trend toward an inverse relationship between total cortisol output during the TSST (AUC_G) and [^{11}C]GR103545 V_T. This is consistent with our *a priori* hypothesis, and agrees with inverse correlations previously reported between [^{11}C]LY2795050 V_T and 24-hour urinary cortisol levels (Pietrzak et al., 2014). Both TSST salivary cortisol AUC_G and 24-hour urinary cortisol reflect HPA tone. While this finding cannot speak to causality, a possible interpretation is that HPA axis tone may regulate dynorphin levels in humans, and thereby affect KOR binding, either through homeostatic mechanisms or through direct competition for radioligand binding. This would be consistent with findings of corticotropin-releasing-factor-mediated dynorphin release in animals (Land et al., 2008). However the observed trend of inverse relationship between total cortisol output during the TSST (AUC_G) and [^{11}C]GR103545 V_T should be interpreted with caution given the small sample size and trend-level finding, and requires examination in a larger sample. We did not observe a relationship between [^{11}C]GR103545 V_T and cortisol reactivity during the TSST, as measured by the AUC_i controlling for baseline cortisol levels. Of note, participants underwent a modified/attenuated form of the TSST that was developed for use in vulnerable populations (individuals with suicidal ideation and children), in which the confederates do not provide negative feedback to the participant during the procedures, but rather maintain neutral facial expressions. This lesser magnitude of the social stressor may have contributed to the lack of longitudinal change in cortisol values at the group level (F=0.79, DF=4, p=0.54), which in turn diminished power to detect relationship between KOR binding and TSST cortisol reactivity (AUC_i).

Sex effects:

We did not observe an effect of sex on V_T, in contrast to a previous study that reported higher KOR binding across multiple regions in males using PET with [^{11}C]LY2795050 and

the same outcome measure (Vijay et al., 2016). This may be related to differences in radiotracer characteristics or to samples studied.

Limitations

The main limitation of the current pilot study is sample size, which was powered to detect large effect sizes, and risked type II error. Life stress measures used in the current study are retrospective self-reports; future studies may consider real-time measurements such as ecologic momentary assessment. Additional technical limitations of this study include the low specific binding of [^{11}C]GR103545 in two *a priori* ROIs, hippocampus or raphe nuclei, and the poor test-retest reliability of [^{11}C]GR103545 V_T in a third ROI, amygdala (Naganawa et al., 2014).

Anatomically proximal subnuclei within ventral striatum exhibit divergent functional effects when KOR are stimulated: KOR agonist administration induces hedonic responses in rats when injected within the rostrodorsal quadrant of the medial shell in nucleus accumbens (1mm^3 in rats), but reduces hedonic responses when injected within the caudal half of the medial shell (Castro and Berridge, 2014). A convergent study in mice using an optogenetic approach identified a parallel divergence between aversive and reinforcing effects of KOR activation in ventral vs. dorsal nucleus accumbens (Al-Hasani et al., 2015). Given this close proximity of sub-nuclei of the ventral striatum with functionally divergent responses to KOR stimulation it is possible that divergent KOR effects may be averaged out within the ventral striatum ROI used in this study, and that such effects, if present in humans, may not be fully dissociable at the resolution of currently available PET imaging.”

Given the role of dynorphin/KOR interactions in modulating activity of both dopaminergic and non-dopaminergic neurons in VTA (Polter et al., 2017), quantification of KOR in VTA in humans would be of significant interest. However, VTA quantification is challenging with [^{11}C]GR103545 given the small volume of this structure and the low PET signal observed in this region.

We selected an agonist radiotracer for this study, which should in theory bind preferentially to KOR in the high-affinity, active state (Wu et al., 2012), and may be sensitive to endogenous dynorphin tone, as suggested in a study with cocaine-use disorder (Diana Martinez, personal communication). However, [^{11}C]GR103545 is limited by suboptimal test-retest reliability and its slow kinetics (Naganawa et al., 2014), which are improved with newer KOR agonist radiotracers (Naganawa et al., 2017).

All KOR radiotracers are limited by the lack of reference region devoid of KOR to allow for quantification of non-specific binding in the brain (V_{ND}). The outcome measure used in this study, V_T, reflects both specific- and non-specific radiotracer binding in target ROIs. Ongoing work to estimate V_{ND} in the absence of a reference region may allow for estimation of binding potential measures for KOR radiotracers in the future (Zanderigo et al., 2017), increasing signal-to-noise ratio and power. Moreover, a previous blocking study with the radiotracer used in this study, [^{11}C]GR103545, estimated a V_{ND} value for this radiotracer of 3.4 (Naganawa et al., 2014). As V_T values in the current dataset in *a priori*

ROIs were in the range of 7.3–19.8, the specific binding fraction of the signal across regions was 53–83% of total V_T, assuming comparable V_{ND} values in our sample.

Conclusions

We did not observe a significant effect of MDD diagnosis on [^{11}C]GR103545 V_T in this initial pilot study. We did observe a trend-level inverse relationship between cortisol tone and [^{11}C]GR103545 V_T. Future studies with larger sample sizes and inclusion strategies targeting depressed populations at increased risk for a kappa opioid abnormality, including those with MDD with psychotic features and those with substance use disorders in early abstinence, are warranted.

Acknowledgments

The authors would like to thank Dr. Mika Naganawa for guidance regarding modeling of the [^{11}C]GR103545 radiotracer.

Funding and Disclosure

NIMH R21MH091553, NIH T35 AG044303, NIH UL1 TR000040

This publication was supported by the National Center for Advancing Translational Sciences, National Institutes of Health, through Grant Number UL1 TR000040. The content is solely the responsibility of the authors and does not necessarily represent the official views of the NIH.

References

Al-Hasani R, McCall JG, Shin G, Gomez AM, Schmitz GP, Bernardi JM, Pyo C-O, Park SI, Marcinkiewcz CM, Crowley NA, Krashes MJ, Lowell BB, Kash TL, Rogers JA, Bruchas MR. 2015 Distinct Subpopulations of Nucleus Accumbens Dynorphin Neurons Drive Aversion and Reward. Neuron 87(5):1063–1077. [PubMed: 26335648]

Ametamey SM, Kessler LJ, Honer M, Wyss MT, Buck A, Hintermann S, Auberson YP, Gasparini F, Schubiger PA. 2006 Radiosynthesis and preclinical evaluation of 11C-ABP688 as a probe for imaging the metabotropic glutamate receptor subtype 5. J Nucl Med 47(4):698–705. [PubMed: 16595505]

Ashburner J, Friston KJ. 2005 Unified segmentation. Neuroimage 26(3):839–851. [PubMed: 15955494]

Avants B, Tustison N, Wu J, Cook P, Gee J. 2011a An open source multivariate framework for n-tissue segmentation with evaluation on public data. Neuroinformatics 9(4):381–400. [PubMed: 21373993]

Avants BB, Tustison NJ, Song G, Cook PA, Klein A, Gee JC. 2011b A reproducible evaluation of ANTs similarity metric performance in brain image registration. Neuroimage 54(3):2033–2044. [PubMed: 20851191]

Beck AT, Kovacs M, Weissman A. 1979 Assessment of suicidal intention: the Scale for Suicide Ideation. J Consult Clin Psychol 47(2):343–352. [PubMed: 469082]

Beck AT, Ward CH, Mendelson M, Mock J, Erbauh J. 1961 An inventory for measuring depression. . Arch Gen Psychiatry 4:3–63.

Berger B, Rothmaier AK, Wedekind F, Zentner J, Feuerstein TJ, Jackisch R. 2006 Presynaptic opioid receptors on noradrenergic and serotonergic neurons in the human as compared to the rat neocortex. British journal of pharmacology 148(6):795–806. [PubMed: 16751796]

Bernstein DP, Fink L. 1998 Childhood trauma questionnaire: A retrospective self-report. San Antonio: The Psychological Corporation.

Bruchas MR, Land BB, Chavkin C. 2009 The dynorphin/kappa opioid system as a modulator of stress-induced and pro-addictive behaviors. Brain Res.

Carlezon WA Jr., Beguin C, DiNieri JA, Baumann MH, Richards MR, Todtenkopf MS, Rothman RB, Ma Z, Lee DY, Cohen BM 2006 Depressive-like effects of the kappa-opioid receptor agonist salvinorin A on behavior and neurochemistry in rats. J Pharmacol Exp Ther 316(1):440–447. [PubMed: 16223871]

Castro DC, Berridge KC. 2014 Opioid Hedonic Hotspot in Nucleus Accumbens Shell: Mu, Delta, and Kappa Maps for Enhancement of Sweetness “Liking” and “Wanting”. The Journal of Neuroscience 34(12):4239–4250. [PubMed: 24647944]

Chavkin C, Koob GF. 2016 Dynorphin, Dysphoria, and Dependence: the Stress of Addiction. Neuropsychopharmacology 41(1):373–374.

Chen Y, Chen C, Wang Y, Liu-Chen LY. 2006 Ligands regulate cell surface level of the human kappa opioid receptor by activation-induced down-regulation and pharmacological chaperone-mediated enhancement: differential effects of nonpeptide and peptide agonists. J Pharmacol Exp Ther 319(2):765–775. [PubMed: 16882876]

Delorenzo C, Delaparte L, Thapa-Chhetry B, Miller J, Mann J, Parsey RV. 2013 Prediction of selective serotonin reuptake inhibitor response using diffusion-weighted MRI. Frontiers in Psychiatry 4.

DeLorenzo C, DellaGioia N, Bloch M, Sanacora G, Nabulsi N, Abdallah C, Yang J, Wen R, Mann JJ, Krystal JH, Parsey RV, Carson RE, Esterlis I. 2015 In vivo ketamine-induced changes in [(1)(1)C]ABP688 binding to metabotropic glutamate receptor subtype 5. Biol Psychiatry 77(3):266–275. [PubMed: 25156701]

DeLorenzo C, Klein A, Mikhno A, Gray N, Zanderigo F, Mann JJ, Parsey RV. 2009 A new method for assessing PET-MRI coregistration. SPIE Medical Imaging Florida, USA p. 72592W-72592W-72598.

Ehrich E, Turncliff R, Du Y, Leigh-Pemberton R, Fernandez E, Jones R, Fava M. 2015 Evaluation of opioid modulation in major depressive disorder. Neuropsychopharmacology 40(6):1448–1455. [PubMed: 25518754]

First M, Spitzer R, Gibbon M, Williams J. 1995 Structured Clinical Interview for DSM-IV Axis I Disorders (SCID-I/P, Version 2.0). New York: Biometrics Research Dept., New York State Psychiatric Institute.

Hamilton M. 1960 A rating scale for depression. J Neurol Neurosurg Psych 23:56–62.

Jin X, Mulnix T, Gallezot JD, Carson RE. 2013 Evaluation of motion correction methods in human brain PET imaging--a simulation study based on human motion data. Medical physics 40(10):102503.

Jordan BA, Cvejic S, Devi LA. 2000 Kappa opioid receptor endocytosis by dynorphin peptides. DNA Cell Biol 19(1):19–27. [PubMed: 10668788]

Keller J, Flores B, Gomez RG, Solvason HB, Kenna H, Williams GH, Schatzberg AF. 2006 Cortisol circadian rhythm alterations in psychotic major depression. Biol Psychiatry 60(3):275–281. [PubMed: 16458262]

Kirschbaum C, Pirke KM, Hellhammer DH. 1993 The ‘Trier Social Stress Test’--a tool for investigating psychobiological stress responses in a laboratory setting. Neuropsychobiology 28(1–2):76–81. [PubMed: 8255414]

Kreibich A, Reyes BA, Curtis AL, Ecke L, Chavkin C, Van Bockstaele EJ, Valentino RJ. 2008 Presynaptic inhibition of diverse afferents to the locus ceruleus by kappa-opiate receptors: a novel mechanism for regulating the central norepinephrine system. J Neurosci 28(25):6516–6525. [PubMed: 18562623]

Land BB, Bruchas MR, Lemos JC, Xu M, Melief EJ, Chavkin C. 2008 The dysphoric component of stress is encoded by activation of the dynorphin kappa-opioid system. J Neurosci 28(2):407–414. [PubMed: 18184783]

Li JG, Zhang F, Jin XL, Liu-Chen LY. 2003 Differential regulation of the human kappa opioid receptor by agonists: etorphine and levorphanol reduced dynorphin A- and U50,488H-induced internalization and phosphorylation. J Pharmacol Exp Ther 305(2):531–540. [PubMed: 12606694]

Mague SD, Pliakas AM, Todtenkopf MS, Tomasiewicz HC, Zhang Y, Stevens WC Jr., Jones RM, Portoghese PS, Carlezon WA Jr. 2003 Antidepressant-like effects of kappa-opioid receptor antagonists in the forced swim test in rats. J Pharmacol Exp Ther 305(1):323–330. [PubMed: 12649385]

McGrath PJ, Miller JM. 2015 Pharmacological Management of Treatment-Resistant Unipolar Depression In: Tasman A, Kay J, Lieberman JA, First MB, Riba MB, editors. Psychiatry. Fourth edition ed: Wiley p. 2311–2330.

McLaughlin JP, Li S, Valdez J, Chavkin TA, Chavkin C. 2006 Social defeat stress-induced behavioral responses are mediated by the endogenous kappa opioid system. Neuropsychopharmacology 31(6):1241–1248. [PubMed: 16123746]

McLaughlin JP, Marton-Popovici M, Chavkin C. 2003 Kappa opioid receptor antagonism and prodynorphin gene disruption block stress-induced behavioral responses. J Neurosci 23(13):5674–5683. [PubMed: 12843270]

Milak MS, DeLorenzo C, Zanderigo F, Prabhakaran J, Kumar JS, Majo VJ, Mann JJ, Parsey RV. 2010 In vivo quantification of human serotonin 1A receptor using 11C-CUMI-101, an agonist PET radiotracer. Journal of nuclear medicine : official publication, Society of Nuclear Medicine 51(12):1892–1900.

Nabulsi NB, Zheng MQ, Ropchan J, Labaree D, Ding YS, Blumberg L, Huang Y. 2011 [11C]GR103545: novel one-pot radiosynthesis with high specific activity. Nuclear medicine and biology 38(2):215–221. [PubMed: 21315277]

Naganawa M, Jacobsen LK, Zheng MQ, Lin SF, Banerjee A, Byon W, Weinzimmer D, Tomasi G, Nabulsi N, Grimwood S, Badura LL, Carson RE, McCarthy TJ, Huang Y. 2014 Evaluation of the agonist PET radioligand [(1)(1)C]GR103545 to image kappa opioid receptor in humans: kinetic model selection, test-retest reproducibility and receptor occupancy by the antagonist PF-04455242. Neuroimage 99:69–79. [PubMed: 24844744]

Naganawa M, Li S, Nabulsi N, Lin S, Labaree D, Ropchan J, Gao H, Henry S, Matuskey D, Carson RE, Huang Y. 2017 Comparison of 11C-EKAP and 11C-FEKAP, two novel agonist PET radiotracers for imaging the kappa opioid receptor in humans. Journal of Nuclear Medicine 58(S1):357. [PubMed: 28153954]

Nemeroff CB, Vale WW. 2005 The neurobiology of depression: inroads to treatment and new drug discovery. J Clin Psychiatry 66 (Suppl 7):5–13.

Newton SS, Thome J, Wallace TL, Shirayama Y, Schlesinger L, Sakai N, Chen J, Neve R, Nestler EJ, Duman RS. 2002 Inhibition of cAMP response element-binding protein or dynorphin in the nucleus accumbens produces an antidepressant-like effect. J Neurosci 22(24):10883–10890.

Ogden RT. 2003 Estimation of kinetic parameters in graphical analysis of PET imaging data. Statistics in medicine 22(22):3557–3568. [PubMed: 14601019]

Ogden RT, Tarpey T. 2006 Estimation in regression models with externally estimated parameters. Biostatistics 7(1):115–129. [PubMed: 16020616]

Oquendo MA, Halberstam B, Mann JJ. 2003 Risk factors for suicidal behavior: the utility and limitations of research instruments In: First MB, editor. Standardized Evaluation in Clinical Practice. Arlington, VA: American Psychiatric Publishing p. 103–130.

Paykel ES. 1997 The Interview for Recent Life Events. Psychol Med 27(2):301–310. [PubMed: 9089823]

Pfeiffer A, Brantl V, Herz A, Emrich HM. 1986 Psychotomimesis mediated by kappa opiate receptors. Science (New York, NY 233(4765):774–776.

Pietrzak RH, Naganawa M, Huang Y, Corsi-Travali S, Zheng MQ, Stein MB, Henry S, Lim K, Ropchan J, Lin SF, Carson RE, Neumeister A. 2014 Association of in vivo kappa-opioid receptor availability and the transdiagnostic dimensional expression of trauma-related psychopathology. JAMA Psychiatry 71(11):1262–1270. [PubMed: 25229257]

Placzek MS, Van de Bittner GC, Wey HY, Lukas SE, Hooker JM. 2015 Immediate and Persistent Effects of Salvinorin A on the Kappa Opioid Receptor in Rodents, Monitored In Vivo with PET. Neuropsychopharmacology 40(13):2865–2872. [PubMed: 26058662]

Polter AM, Barcomb K, Chen RW, Dingess PM, Graziane NM, Brown TE, Kauer JA. 2017 Constitutive activation of kappa opioid receptors at ventral tegmental area inhibitory synapses following acute stress. eLife 6.

Pruessner JC, Kirschbaum C, Meinlschmid G, Hellhammer DH. 2003 Two formulas for computation of the area under the curve represent measures of total hormone concentration versus time-dependent change. Psychoneuroendocrinology 28(7):916–931. [PubMed: 12892658]

Schatzberg AF. 2015 Anna-Monika Award Lecture, DGPPN Kongress, 2013: the role of the hypothalamic-pituitary-adrenal (HPA) axis in the pathogenesis of psychotic major depression. World J Biol Psychiatry 16(1):2–11. [PubMed: 24933348]

Schoultz BW, Hjornevik T, Willoch F, Marton J, Noda A, Murakami Y, Miyoshi S, Nishimura S, Arstad E, Drzezga A, Matsunari I, Henriksen G. 2010 Evaluation of the kappa-opioid receptor-selective tracer [(11)C]GR103545 in awake rhesus macaques. Eur J Nucl Med Mol Imaging 37(6):1174–1180. [PubMed: 20157708]

Shirayama Y, Ishida H, Iwata M, Hazama GI, Kawahara R, Duman RS. 2004 Stress increases dynorphin immunoreactivity in limbic brain regions and dynorphin antagonism produces antidepressant-like effects. J Neurochem 90(5):1258–1268. [PubMed: 15312181]

Talbot PS, Narendran R, Butelman ER, Huang Y, Ngo K, Slifstein M, Martinez D, Laruelle M, Hwang DR. 2005 11C-GR103545, a radiotracer for imaging kappa-opioid receptors in vivo with PET: synthesis and evaluation in baboons. J Nucl Med 46(3):484–494. [PubMed: 15750163]

Tao R, Auerbach SB. 2002 Opioid receptor subtypes differentially modulate serotonin efflux in the rat central nervous system. J Pharmacol Exp Ther 303(2):549–556. [PubMed: 12388635]

Tomasi G, Nabulsi N, Zheng M-Q, Weinzimmer D, Ropchan J, Blumberg L, Brown-Proctor C, Ding Y-S, Carson RE, Huang Y. 2013 Determination of In Vivo Bmax and Kd for 11C-GR103545, an Agonist PET Tracer for κ-Opioid Receptors: A Study in Nonhuman Primates. Journal of Nuclear Medicine.

Vijay A, Wang S, Worhunsky P, Zheng MQ, Nabulsi N, Ropchan J, Krishnan-Sarin S, Huang Y, Morris ED. 2016 PET imaging reveals sex differences in kappa opioid receptor availability in humans, in vivo. American journal of nuclear medicine and molecular imaging 6(4):205–214. [PubMed: 27648372]

Wang Y, Xu W, Huang P, Chavkin C, Van Bockstaele EJ, Liu-Chen LY. 2009 Effects of acute agonist treatment on subcellular distribution of kappa opioid receptor in rat spinal cord. J Neurosci Res 87(7):1695–1702. [PubMed: 19130621]

WHO. 2017 Depression and other common mental disorders: global health estimates. In: Organization. WH, editor. Geneva: World Health Organization p. 1–24.

Wu H, Wacker D, Mileni M, Katritch V, Han GW, Vardy E, Liu W, Thompson AA, Huang XP, Carroll FI, Mascarella SW, Westkaemper RB, Mosier PD, Roth BL, Cherezov V, Stevens RC. 2012 Structure of the human kappa-opioid receptor in complex with JDTic. Nature 485(7398):327–332. [PubMed: 22437504]

Wu S, Ogden RT, Mann JJ, Parsey RV. 2007 Optimal metabolite curve fitting for kinetic modeling of 11C-WAY-100635. J Nucl Med 48(6):926–931. [PubMed: 17504866]

Zanderigo F, Mann JJ, Ogden RT. 2017 A hybrid deconvolution approach for estimation of in vivo non-displaceable binding for brain PET targets without a reference region. PloS one 12(5):e0176636.

Zanderigo F, Ogden RT, Bertoldo A, Cobelli C, Mann JJ, Parsey RV. 2010 Empirical Bayesian estimation in graphical analysis: a voxel-based approach for the determination of the volume of distribution in PET studies. Nuclear medicine and biology 37(4):443–451. [PubMed: 20447556]

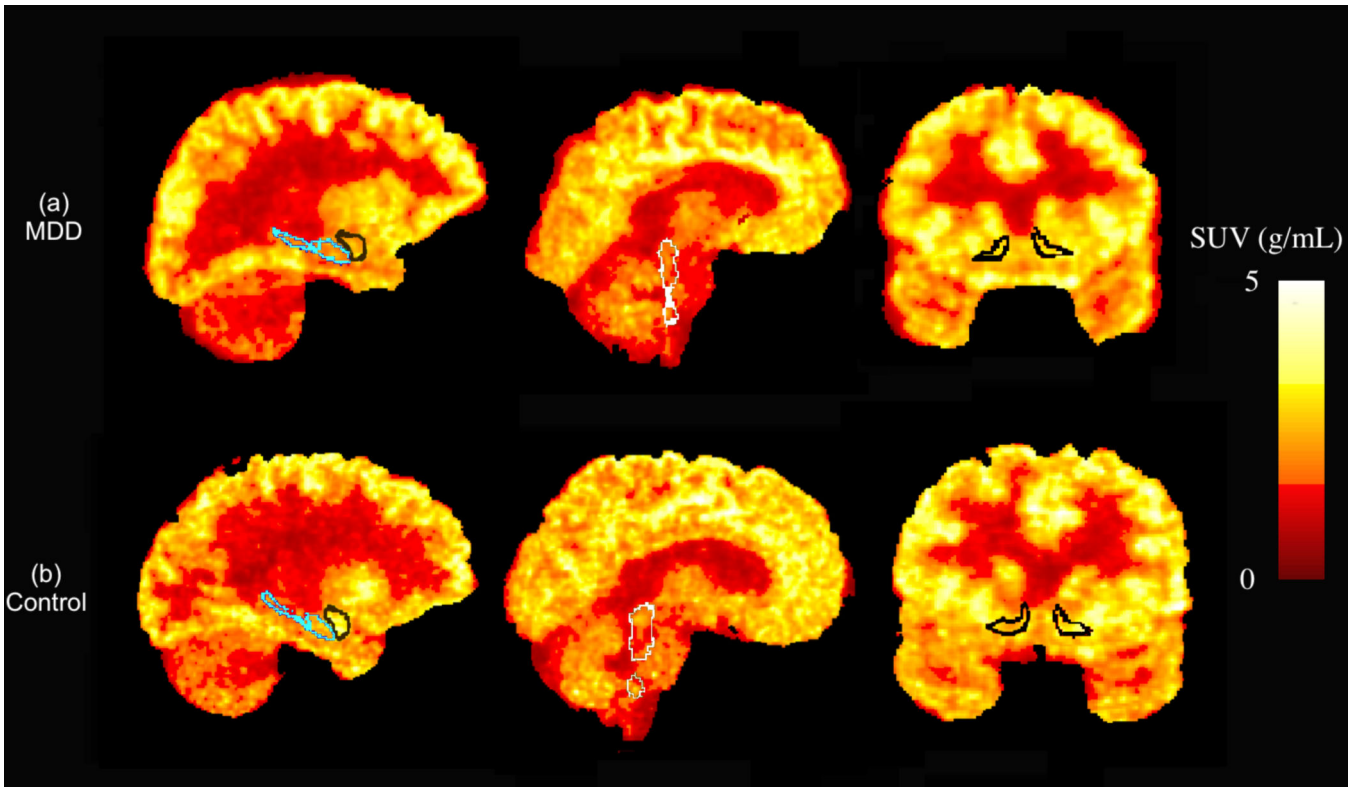

Figure 1.

Representative single-subject whole-brain images to demonstrate distribution of [^{11}C]GR103545 binding. [^{11}C]GR103545 Standard Uptake Values (SUV) (unmodeled data) from two individuals whose V_T values were at the medians of the (a) MDD and (b) healthy volunteer samples, respectively, demonstrating expected distribution of KOR. Outlines of *a priori* regions of interest are superimposed on images (amygdala: black, left panel; hippocampus: blue, left panel; raphe nuclei: white, center panel; ventral striatum: black, right panel).

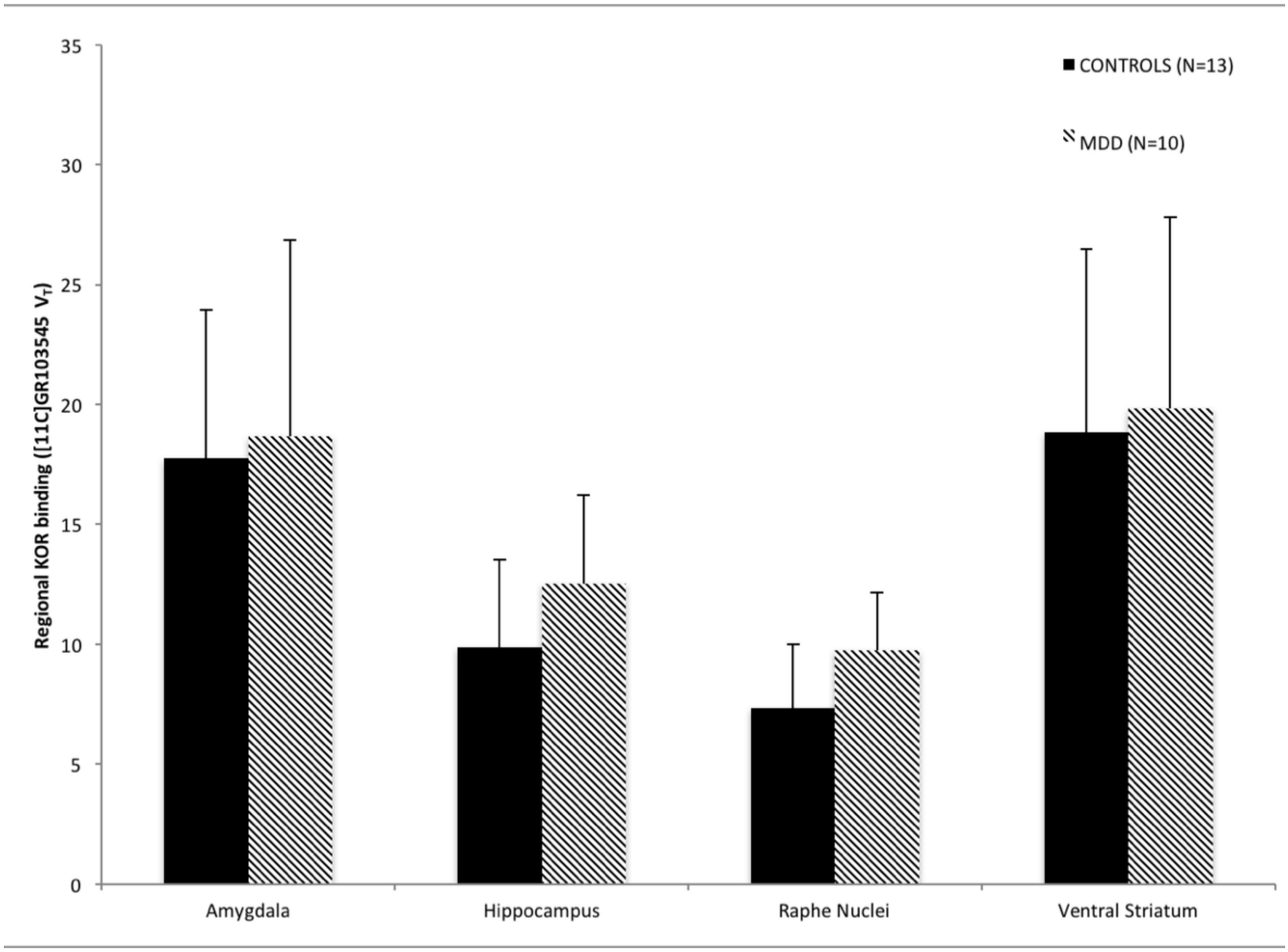

Figure 2.

Comparison of [^{11}C]GR103545 V_T between MDD and healthy volunteer groups across four *a priori* regions of interest: amygdala, hippocampus, raphe nuclei, and ventral striatum. Bar heights represent the weighted means for each region of interest. Error bars indicate the corresponding standard deviations of the weighted means. No significant difference is observed (p=0.48).

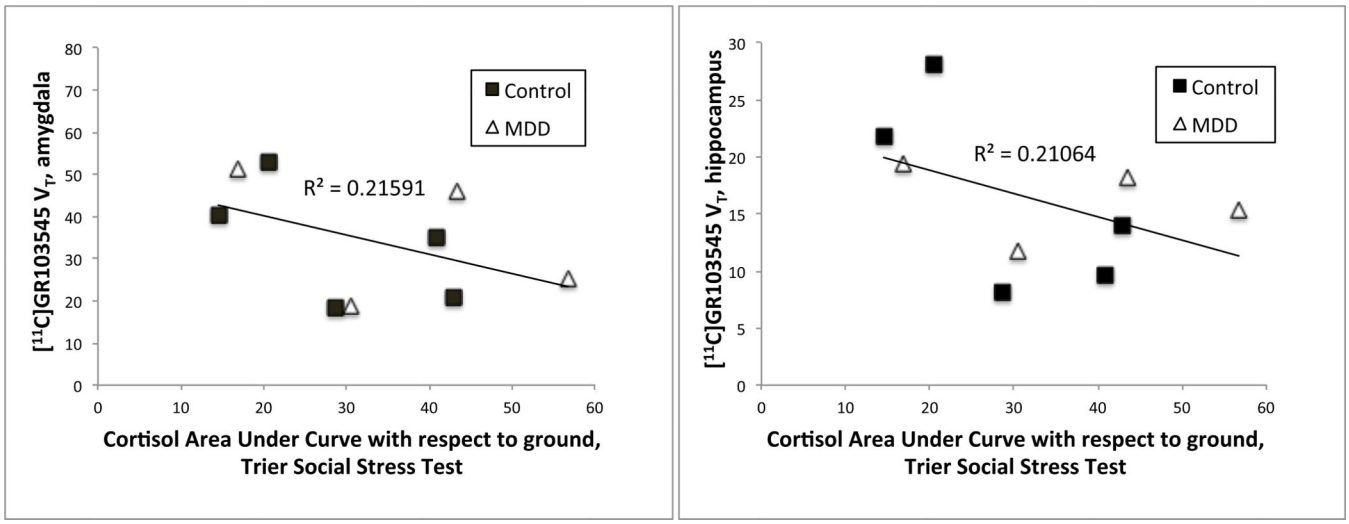

Figure 3.

Relationship of cortisol output during the modified Trier Social Stress Test to [^{11}C]GR103545 V_T. Inverse relationship was observed at a trend level considering four *a priori* regions of interest (p=0.081 amygdala, hippocampus, raphe nuclei, and ventral striatum). Amygdala and hippocampus are demonstrated in this figure.

Table 1.

Clinical and Demographic Information

	Controls(N=13)	MDD (N=10)	*p-value (Control vs MDD, 2-tailed t-test)*
Age	34.8±10	32.6±6.5	0.54
Hamilton Depression Rating Scale (24-item)	0.7±1.1	25.7±6	< 0.001
Beck Depression Inventory	0.2±0.6	29.3±10.2	< 0.001
Years of Education	13.7±6.9	15.3±1.4	0.48
Age at Onset	N/A	12.8±9	N/A
Number of Negative Life Events	0.1±0.3	1.6±1.4	0.001
Childhood Trauma Questionnaire Total Score	32±8.3	47±9	< 0.001
Injected Dose (mCi)	11.6±4.1	11.3±6	0.88
Injected Mass (μg)	0.4±0.3	0.5±0.3	0.5
		Median (Range)	
Number of Previous Depressive Episodes	N/A	1 (8)	N/A
Length of Current Major Depressive Episode (days)	N/A	27 (789)	N/A
Categorical Variables	**N (%)**		**p-value (Control vs MDD, fisher's extact)**
Female	6 (46.2)	5 (50)	1
Subjects With a History of Major Depression in First Degree Relatives	0 (0)	2 (20)	
Subjects with a Comorbid Anxiety Disorder	0 (0)	2 (20)	
Subjects with a Comorbid Dysthymia	0 (0)	1 (10)	
Subjects with Current Suicidal Ideation	0 (0)	5 (50)	
Race/Ethnicity			
Asian	1 (8)	1 (10)	
African American	3 (23)	2 (20)	
Caucasian	7 (54)	5 (50)	
Hispanic	1 (8)	1 (10)	
>1 Race	1 (8)	1 (10)	